Journal of Harbin Engineering University
ISSN: 1006-7043

Vol 45 No. 9
September 2024

FEM Analysis of Light Weight RC Beams Made Using Expanded Polystyrene and Montmorillonite

Surjith Singh Raja R P, J. Saravanan
Research Scholar, Department of Civil and Structural Engineering, Annamalai University, Chidambaram, India
Associate Professor, Department of Civil and Structural Engineering, Annamalai University, Chidambaram, India

Abstract
Owing to advancements in technology and research on the compressive strength of concrete in recent years, light weight concrete (LWC) has emerged as the material of choice for applications requiring economy, high strength, stiffness, and durability. Nonetheless, ductility and strength are typically inversely correlated. Under severe applied loads, lightweight concrete can suddenly break due to its brittle nature. Lightweight concrete composed of cement, calcined montmorillonite powder, natural coarse aggregate, expanded polystyrene, sand, and water was used in this investigation. Investigating the nonlinear flexural behaviour of reinforced lightweight concrete (RLWC) beams is the goal of this work. The ANSYS software was utilized to create finite element models, investigating the impact of various factors on the flexure response of RLWC beams. The main steel's impact and yield strength, as well as the beam's breadth, depth, and shear span, are among the factors taken into account. The resulting outcomes were compared with the outcomes of the experiment. By utilizing FEA at the same location as the experimental test of the beam, the load deflection curve was determined.
Keywords: Lightweight concrete, reinforced concrete beam, flexural behaviour, ANSYS, Finite Element.

1. Introduction

The development of lightweight aggregate concrete (LWC) has received a lot of attention since it has many superior qualities over regular weight concrete, such as lower density, improved fire resistance, higher earthquake resistance, and more. However, a few flaws with LWCs, like a poor tension-compression ratio and reduced tensile and shear strength, have kept them from being widely utilized in the building sector. We are well aware that adding fibers to concrete can mitigate these negative consequences and significantly increase the ductility and strength of LWCs. Fibres of various types can be added to concrete, particularly light-weight combinations, to boost the material's ability to absorb energy after matrix breaking. Fibres decrease the crack opening in a material, increasing its fatigue strength [1]. In cyclically stressed fibre reinforced concrete, the specimen's maximum deformation and the width of the matrix rupture fracture affect the post-cracking zone's elasticity modulus. This is due to the fact that these two elements play a part in the matrix's rupture. More energy is needed in fiber-reinforced concrete to overcome reinforcing mechanisms after the matrix breaks than is consumed during matrix breakdown. Thus, energy absorption capacity is the main benefit of fibre reinforcement [2]. A further consequence of the growing demand for living space in modern architecture is their increased height, depth, and width [3]. To meet these demands, new, extremely strong, lightweight concrete has been developed throughout the last 20 years [4,5].

To improve LWC's tensile and flexural strength, resilience to quick and dynamic loading, and ability to withstand explosive impacts, steel fibers are added. By including steel fibers, LWFC's ability to support weight is increased to the level of conventional weight concrete's strength. This reduces the width of the cracks and regulates how they spread. Furthermore, by lowering the weight of the concrete, the potential to deform is reduced, leading to cost-effective solutions [6,7]. To examine the flexural characteristics of concrete reinforced with fibres, many studies, both theoretical and practical, have been conducted. A theoretical discussion of steel fiber reinforced concrete was conducted by Solahuddin [8]. An inquiry into the application of fiber-reinforced polymer composite in improving the structural behavior of reinforced concrete beams was carried out by Solahuddin & Yahaya [9]. Zhu et al. [10] investigated the application of ultra-high-performance concrete for

flexural support of reinforced concrete structures. Khaleel [11] looked into how steel fibers affected the flexural strength, crack lengths, and shear strength of concrete beams under repeated stress. Steel fiber's effect on flexural toughness in self-compacting lightweight aggregate concrete was investigated by Li et al. [12]. In order to disperse short, thin steel fibers in ultra-high-performance concrete, Gou et al. [13] created a unique technique. A study by Mohamed et al. [14] investigated how steel fiber affected the deep beams' resistance to deterioration composed of lightweight reinforced concrete foam. Similar flexural response to normal weight concrete was found by Alshannag et al. [15] when they investigated the application of naturally occurring lightweight aggregates in the construction of reinforced concrete beams. In an investigation of how glass fiber-reinforced polymers behave in structural buildings, Mohammed et al. [16] discovered that compared to steel, these composites had more cracks and a greater ultimate load capacity. Lightweight concrete beams strengthened with glass-fiber reinforced polymer bars were examined for both their serviceability and flexural behaviour by Mehany et al. [17].

When building a long-span bridge, lightweight aggregate concrete (LWC) has several benefits, such as decreased internal force and expanded beam span. Because of its remarkable ductility and resilience to cracking, Lightweight concrete reinforced with steel fiber is gaining popularity. The researchers had to find less expensive ways to simulate concrete structures because experimental tests are costly and time-consuming. To achieve this, they used a variety of numerical and analytical modeling techniques. When compared to experimental research, finite element (FE) analysis yields precise and expedient results for structural assessment. Many researchers attempt to demonstrate the simpler and easier approach, for as by developing software like ANSYS. This work employs the finite element method and ANSYS to investigate the nonlinear flexural behavior of reinforced lightweight concrete (RLWC) beams. The outcomes were then compared with experimental findings.

2. Literature Survey

Touhami Tahenni et al., [18] examined how steel fibers affected the deflection behavior and stiffness of tensioned concrete reinforced with steel. The study compared experimental deflections with theoretical values from popular design codes using four-point bending. A novel model that took into account the steel fiber orientation, aspect ratio, and volume percentage was presented. The study discovered that the stiffness and deflection behavior of tensioned concrete were greatly enhanced by the steel fibre addition. It was discovered that the model could satisfactorily and reliably estimate the SFRC beam deflection.

Mohammad Alshannag et al., [19] examined how lightweight, high-strength concrete beams reinforced with reused plastic fibers, steel, and crimped polypropylene would respond to flexural loads. Comparing fiber-reinforced beams to control beams, the results indicate that the former have higher toughness, ductility, and load carrying ability. With steel fibres (0.5%) and crimped polypropylene fibres (0.25%), the reinforced beams showed the most benefit.

Al-Naimi et al., [20] explored the impact of 3D fibres on recycled lightweight concrete beams, focusing on ductility and flexural behavior. Steel fibres were used to enhance ductility, and stirrups were partially replaced with fibres. Results show fibre reinforcement can partially replace stirrups, but complete removal leads to brittle failure. The study uses nonlinear finite element analysis to validate a SFRLC constitutive model.

Zareef et al., [21] examined the flexural characteristics of GFRP (glass fiber reinforced polymer) bars, which are utilized to strengthen LWCBs, or lightweight concrete beams. It evaluates how well LWCBs perform in comparison to Normal Concrete Beams (NCBs) when they have different GFRP bars and Steel Reinforcement (SR) ratios. Finite element models and beam test results exhibit a strong correlation, according to the results, with GFRP-reinforced LWCBs primarily functioning as elastic deformed elements. This demonstrates the potential of GFRP and LWC bars in the building sector.

Ghannoum et al., [22] examined whether finite element (FE) modelling is a suitable method for predicting how reinforced concrete beams' shear

strength will behave with EPS additions. The experimental load-deflection qualities can be precisely replicated by both FE techniques, according to the results. Nonetheless, the approximate cracked patterns and damaged-zone distribution during loading stages cannot be obtained with the deterministic FE technique. Given the concrete heterogeneity and changed spatial mechanical properties resulting from EPS additions, the stochastic technique makes sense.

Alzara et al., [23] examined how fire-exposed reinforced foam concrete slabs behaved in relation to concentric and eccentric stresses. Using the ANSYS software and the finite element approach, the study examined flat slabs of reinforced concrete that were 150 mm thick and had a density of 1820 kg/m3. Based on the study, foam concrete slabs' maximum bearing weight is reduced by 25% due to fire effect. The study also discovered that the compressive strength of lightweight structural concrete made with fibres and additives was 30.0 MPa and its density was 1820 kg/m3. Lightweight concrete slabs had a low maximum load, a decrease in cracks, and an increase in crack width.

Ibrahim et al., [24] examined the shear behaviour of deep beams under single midspan focused loads utilising polystyrene foam balls in place of some of the coarse material. According to the findings, these beams are 30% lighter than NWC deep beams and exhibit almost the same shear behaviour and failure cause. Cracking and ultimate shear strength are strongly influenced by the shear span-to-depth ratio; bigger values result in lower ultimate shear strengths. When there are gaps in the shear span, the ultimate strength decreases, but the ultimate load decreases as the opening depth increases. Shear capacity and displacement ductility are improved when beams surrounding apertures are internally stiffened, and ultimate shear capacity and displacement are enhanced when the proportion of reinforcement made of tensile steel is raised. The research suggests that the opening depth should not exceed 20% of the deep beam depth and internal strengthening is recommended.

Xi Liu et al., [25] examined fourteen light-weight aggregate concrete beams under a four-point bend stress that had fiber-reinforced polymer reinforcement bars. The beams were simple and strengthened with steel fibres. Lowering the largest crack width under light loads was discovered to be possible with steel fiber-reinforced lightweight concrete and longer clear spans; lowering the largest crack width at all loading levels was demonstrated to be possible with higher reinforcing ratios. More over 50% of the samples reinforced with GFRP had non-conservative fracture lengths, even though all CFRP-reinforced beams satisfied the 0.7 mm fracture width criteria. Regarding beams strengthened with GFRP and CFRP, a logical alternative crack width model was presented, taking into account the impacts of steel fibres and lightweight aggregates. The results of the investigation validate the crack width formulae in ACI 440.1R and ISIS-M03, however nearly all of the time GB 50608 provided estimates that were dangerous.

Chandramouli et al., [26] investigated the use of lightweight clay aggregate (LECA) in lightweight concrete (LWC) beams as a complete substitute for coarse aggregate. The LWC beams' energy absorption capability, ductility index, and load-deflection were contrasted with those of conventional concrete beams. The study discovered that LECA can be substituted for stone aggregate in concrete without having an impact on the material's structural integrity. Welded wire mesh (WWM) was used as internal reinforcement to boost load carrying capacity without adding weight to the beam. The study also discovered that the increased binder content in LWC concrete can be offset by using fly ash.

Al Zand et al. [27] evaluated a novel steel-concrete composite beam system's flexural performance for flooring applications. System preparation involves filling a cold-formed steel C-section with concrete that contains a range of lightweight recycled aggregates. 14 samples of galvanised steel C-purlin, both with and without the filler material, were evaluated for the investigation. The findings demonstrated that performances in terms of ductility, bending capacity, and flexural stiffness were greatly enhanced while varying the percentage of recycled aggregates filled in the C-sections. Additionally, stiffening the composite using screw connectors or steel strips enhanced its behaviour and raised its bending capacities.

3. Proposed Materials And Methodologies

A. Materials and mix proportions

In order to create lightweight concrete for the purposes of this experiment, EPS and montmorillonite were partially substituted for traditional granite aggregates and cement. Cement, montmorillonite, fine and coarse aggregate, EPS, super plasticizer (SP), and water were the ingredients in the mixture. The montmorillonite replacement at 0, 2 and 4 % by the weight of cement were used. EPS as replacement for coarse aggregate at 10% was used. The 4 kinds of LWC mixes were used to create reinforced light weight concrete beam, they are conventional concrete (CC) mix, 10E mix (10% EPS), 2M10E mix (2% montmorillonite & 10% EPS) and 4M10E mix (4% montmorillonite & 10% EPS).

Reinforced concrete beam details

Four beams in total were built and tested. The beams were intended to be under-reinforced. Every beam had the same dimensions: 240 x 120 x 1200 mm. Each beam was reinforced flexurally at the bottom by two 8mm diameter bars and shearly at the top by two 6mm diameter bars. The stirrups were spaced 150 mm c/c.

B. Finite Element Analysis

SolidWorks software generates a solid rectangular beam model using a parametric feature-based methodology. The model includes dimensions, bar diameter and length, stirrups, and holes. The model is assembled with reinforced bars and stirrups using SolidWorks' "mate" option. Load and support positions are marked on the model, allowing for simple supported ends. The model is stored in IGES format for easy import into ANSYS. The geometric beam model is displayed in Figures 1 & 2.

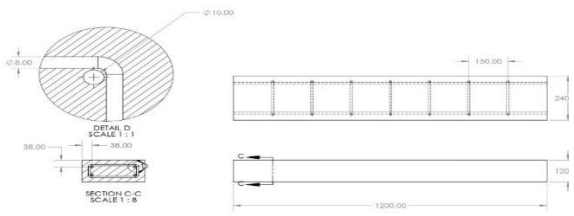

Fig.1. Dimension of beam model

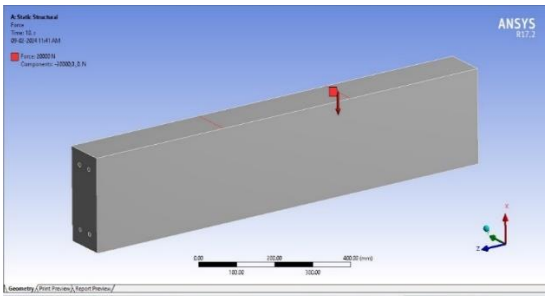

Fig. 2. Geometrical beam model designed in SolidWorks

Static structural

The required model in ANSYS is subjected to a range of evaluations, encompassing structural studies that are static, dynamic, fluid flow, and thermal. While dynamic structural analysis looks at a model under dynamic pressures that vary with time or frequency, static structural analysis looks at a fixed body under a constant load. A liquid or gas passing through or around an object is simulated in the study of fluid flow. Similarly, the body was subjected to thermal examination in order to ascertain how temperature affected the material's characteristics. In this experiment, the RLWC beam acted as a stationary body under static pressures. For that reason, a static structural analysis was performed on the developed beam model.

Engineering data

This stage involved importing the properties of the various LWC mixtures (CC, 10E, 2M10E, and 4M10E) into the ANSYS program. The Young modulus, density, and ratio of Poisson's values for the various LWC mixes are shown in Table 1. The ANSYS program also included the data for the steel's density, steel grade, Young's modulus and Poisson's ratio.

Table 1: Aspects Of Various Concrete Mixes

Mix ID	Density (kg/m^3)	Elasticity modulus, (GPa)	Poisson's ratio
Concrete	41500	45000	0.15
Reinforced steel	7850	200000	0.30

Model

At this point, the different parts of the model have been given the steel properties and the experimental features of the various LWC mixes

(10E, 2M10E, and 4M10E), such as density, Young's modulus, and Poisson's ratio values. The links between the different parts of a model have been observed, and any discrepancies found will be fixed at this phase. The geometric model is now divided into several parts using tetrahedron meshing. The mesh size and type needed for the built model were fine, medium, and coarse. The RLWC beam was represented in this work using a fine mesh type. The tetrahedron meshing of the beam model is shown in Fig. 3.

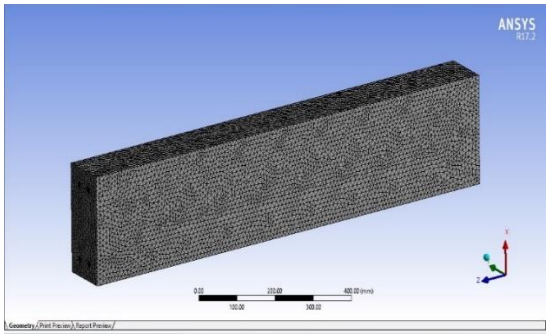

Fig. 3. Tetrahedron meshing of beam model

Geometry And Loading Conditions

The overall length of a simply supported beam is 1200 mm. The size of beam is 120 x 240 mm. Beam loaded equally from two locations at one-third of the span points away from the support. As seen in figure 3, mesh size was taken into consideration with an edge length of 10 mm to ensure accuracy of findings.

Six-millimeter bars are used to construct the stirrups, while eight and six-millimeter deformed bars with high yield strength make up the longitudinal reinforcement. Two HYSD bars, each with an 8 mm diameter, make up the tension reinforcement. As hang-up bars, two mild steel bars measuring 6 mm are also included.

Setup

The required forces (loads) have been applied to the generated model, and the required support conditions have been established for it. In this work, the ultimate loads derived from experimentation were applied to the current models in order to analyse the behaviour of the beam model. The ANSYS-derived deflections and the experimental deflections of the LWC mixtures were compared.

This experiment recorded the directional and total deformations of the beam models. The failure pattern and cracking behaviour of the manufactured models were also observed. The standard, shear, maximum, minimum, and thermal stresses were among the stress parameters that were discovered through the modelling and analysis of the beam element in the ANSYS simulation.

C. Theoretical analysis

Strengthened specimens for shear

The shear capacity Vu of the shear-strengthened material is assessed using the simple superposition technique to determine the effectiveness of lightweight concrete beams reinforced with steel fiber composites.

$$v_u = v_c + v_s + v_f \quad (1)$$

The longitudinal steel reinforcements' shear resistance (Vc) and the transverse steel reinforcements' shear capacity (Vs) may be determined using several design equations for reinforced concrete buildings or by analysing the test results of control beams. For the purpose of creating design standards, it is essential to accurately forecast the shear contribution Vf of steel fibre composites.

According to ECP, the steel fibre composites shear reinforcement's nominal shear strength is provided by

$$q_{fu} = A_f\left(E_f \varepsilon_{ef} / \gamma_f\right)(\sin\alpha + \cos\alpha)\left(d_f / d\right)\left(S_{f^*} b_w\right) \quad (2)$$

$$A_f = 2\mathrm{n}\, t_f w_f \quad (3)$$

$$\varepsilon_{e_f} = 0.75\varepsilon_{fu^*} \leq 0.04 \quad (4)$$

$$\varepsilon_{f_u}^* = CE\varepsilon_{fu} \quad (5)$$

The requirement is that the spacing Sf be less than 200 mm or d/4, whichever is less.

According to (ACI, 2017), The shear reinforcement of steel fibre composites is provided by

$$\frac{v_f = A_{f_v} F_{f_e} (\sin\alpha + \cos\alpha)\, d_{fv}}{s_f} \quad (6)$$

Where

$$A_{f_v} = 2nt_f w_f \quad (7)$$

Tensile stress within the reinforcement is directly correlated with strain in steel fiber composite shear reinforcement at nominal strength.

$$F_{f_e} = \varepsilon_{f_e} E_f \quad (8)$$

In the steel fibre reinforcement, the effective strain is provided by

$$\varepsilon_{f_e} = \min\left(k_v \varepsilon_{f_u}, 0.75\varepsilon_{f_u}, 0.004\right) \quad (9)$$

in which kv, the bond-reduction coefficient is determined using

$$k_v = \frac{k_1 k_2 L_e}{11900\varepsilon_{fu}} \le 0 \cdot 75 \quad (10a)$$

Two modification factors (k1 and k2), which take into consideration the concrete strength and wrapping technique, respectively, are necessary to calculate the bond-reduction coefficient. These factors of modification are provided by

$$k_1 = \left(\frac{f'c}{27}\right)^{2/3} \quad (10b)$$

here the compressive strength of LWC is represented by f ′ c, and

$$k_2 = \frac{d_{fv} - L_e}{d_{fv}} \quad (10c)$$

where the majority of the bond stresses are sustained over the active bond length Le, which is determined by

$$L_e = \frac{23300}{(nt_f E_f)^{0\cdot 58}} \quad (10d)$$

A reinforced element's shear capacity is calculated in fib-TG9.3 using the EC2 format as follows:

$$v_{Rd} = v_{cd} + v_{wd} + v_{fd} \quad (11)$$

where the steel fibre's contribution to the shear capacity Vfd is calculated using

$$V_{fd} = 0 \cdot 90\varepsilon_{f,e} E_f \rho_f b_w d(\cot\theta + \cot\alpha)\sin\alpha \quad (12a)$$

$$\varepsilon_{fe} = \min\left[0.65\left(\frac{fcm^{2/3}}{E_{fu}\rho_f}\right)^{0\cdot 56} \times 10^{-3},\ 0 \cdot 17\left(\frac{f_{cm}^{2/3}}{E_{fu}\rho_f}\right)^{0\cdot 3}\varepsilon_{fu}\right] \quad (12b)$$

The qfu was calculated using Equations (2–5) (ECP, 2005), the Vf was calculated using Equations (6–10) (ACI, 2017), and the Vfd was calculated using Equations 11, 12a, and 12b (FIB, 2001). Using the design codes, every test beam specimen's failure loads were calculated and compared to values found during experimentation. Analytical models will differ from experiment as these programmes do not have the LWC beam's calibration. All of the analytical models, to varying degrees, underestimate the failure load prediction when compared to their experimental equivalents. The impact of the steel fibre strips' width on the analytical outcomes.

Strengthened specimens for flexure

It is crucial to ascertain the degree of strain in the steel fibre reinforcement at the cross section's final moment in ECP, 2005. The strain level created during concrete crushing, steel fiber rupture, or steel fiber debonding from the substrate determines the strain value allowed in steel fiber laminates at section failure (εfe). This strain's value is determined by

$$\varepsilon_{fe} = \varepsilon_{cu}\left(\frac{h-c}{c}\right) - \varepsilon_{bi} \le k_m \varepsilon_{fu}^{*}, \quad (13)$$

Where

$$\varepsilon_{fu}^{*} = CE\varepsilon_{f_u}, \quad (14)$$

Moreover, CE is 0.95.

$$f_{fe} = E_f \varepsilon_{fe} / \gamma_f \quad (15)$$

The failure mode regulating the cross section reinforced with externally bonded steel fiber needs to be considered when performing the computation to determine the ultimate flexural strength. To make sure the conditions for balance and compatibility are met, such a technique necessitates a trial-and-error approach. Through trial and error with particular equations, the stress and strain values of reinforcing steel are determined.

$$\varepsilon_s = \left(\varepsilon_{fe} + \varepsilon_{bi}\right) * \left(\frac{d-c}{h-c}\right) \quad (16)$$

$$f_5 = E_s\varepsilon_s \le f_y / \gamma_s \quad (17)$$

In compressed concrete, the rectangular stress block's depth is established by

$$a = \frac{A_s f_s + A_f f_{fe}}{(0.67 f_{Cu} * b)/\gamma_C} \quad (18)$$

The final flexural moment is determined using

$$M_u = A_s f_s\left(d - \frac{a}{2}\right) + A_f f_{fe}\left(h - \frac{a}{2}\right) \quad (19)$$

For two-point loading, the ultimate load Pu is determined by

$$P_u = \frac{2Mu}{X} \quad (20)$$

where X is the length in millimetres between the loading point and the supports. Based on the strain distribution found in ACI 440.2R-17, the strain level in steel fibre composites, denoted as εf, may be computed for any presumed depth to the neutral axis c by applying the following formula:

$$\varepsilon_f = \varepsilon_{cu}\left(\frac{n-c}{c}\right) \le \varepsilon_{fu} \quad (21)$$

Assuming elastic nature, the stress level in steel fiber composites can be ascertained by comparing the strain level in the steel fiber composites.

$$f_f = E_f\varepsilon_f \quad (22)$$

and the amount of strain in steel under stress εs may be computed using

$$\varepsilon_S = \varepsilon_f\left(\frac{d-c}{h-c}\right) \quad (23)$$

Furthermore, the strain level for steel under compression may be computed using

$$\varepsilon_s' = \varepsilon_f\left(\frac{d'-c}{h-c}\right) \quad (24)$$

Under the assumption of elastic-plastic behavior, the stress level in steel (fs) is found by contrasting the strain level in steel.

$$f_s = E_s \varepsilon_s \quad (25)$$

To verify internal force balance, use

$$C = \frac{A_s f_s + A_f f_f + A_{s'} f_{s'}}{0.85 f_{C'} \beta_1 b} \quad (26)$$

Thus, for concrete with a 35 MPa compressive strength, β1 = 0.8. The compatibility of strain and internal force equilibrium are established by concurrently meeting Eqns. 21, 24, and 26, which yields the actual neutral axis depth, c. With steel fibre composites external reinforcement Mu, the nominal flexural strength of the section may be calculated using

$$M_u = A_s f_s \left(d - \frac{\beta_1 C}{2}\right) + \psi A_f f_f \left(h - \frac{\beta_1 C}{2}\right) + A_{s'} f_{s'} \left(d' - \frac{\beta_1 c}{2}\right) \quad (27)$$

where ψ is equal to 0.85. For two-point loading, the ultimate load Pu is determined by

$$P_u = \frac{2Mu}{X} \quad (28)$$

The most preferred failure mode in FIB, 2001 is concrete smashing and steel yielding, which happens when the concrete is crushed after the tensile steel reinforcement yields, failing the critical cross section. Using RC design principles, the reinforced cross section's design bending moment is computed. Utilizing strain compatibility and internal force equilibrium, the neutral axis depth x is computed to yield the design moment. Since the RC element might not be completely unloaded when strengthening happens, the analysis should take into account the extreme tensile fiber's starting strain, ε◦. Using the following formula, one may determine the design bending moment capability.

1. The neutral axis depth x can be computed as follows:

$$0 \cdot 85 \psi f_{Cd} b_X = A_{s2} E_s \varepsilon_{s2} = A_{s1} f_{yd} + A_f E_{fu} \varepsilon_{fu} \quad (29)$$

where ψ = 0.8 and

$$\varepsilon_{s2} = \varepsilon_{cu} \left(\frac{x - d_2}{x}\right) \quad (30)$$

$$\varepsilon_f = \varepsilon_{Cu} \left(\frac{h - x}{x}\right) - \varepsilon^0 \quad (31)$$

2. Create the following bending moment capacity:

$$M_{Rd} = A_{s1} f_{yd} (d - \delta_{Gx}) + A_f E_f \varepsilon_f (h - S_{Gx}) + A_{s2} E_s \varepsilon_{s2} (\delta_{Gx} - d_2) \quad (32)$$

where 0.4 is the value of δG. For two-point loading, the ultimate load Pu is determined by

$$P_u = \frac{2M_{Rd}}{X} \quad (33)$$

Three analytical models that are produced from design codes are compared with the experimental results in this study. Using Equations 13 to 20 (ECP, 2005), Eqns 21 to 28 (ACI, 2017), and 29 to 33 (FIB, 2001), NWC design algorithms were used to determine and compare the flexural moment and failure loads of reinforced specimens to actual LWC values. ACI, 2017 and FIB, 2001 codes are closer to the outcomes of the experiment, whereas the ECP, 2005 predicts the failure load more accurately but is more conservative when predicting the ultimate load.

4. Results And Discussion

A. Flexural behavior of RLWC beams

The flexural behavior of beam models for the conventional concrete at 50KN are depicted in Fig.4 (a&b) and the beam's maximum deflection and stress values is shown in table 2 and table 3. The mid-span deflection of the CC beam was observed to be 0.891mm, 1.782 mm, 2.673mm, 3.564mm, 4.455mm at a load of 10-, 20-, 30-, 40-, and 50-kN, respectively.

Table 2: Cc Beams' Load-Deflection Values

Load (KN)	Max. deflection (mm)	
	Experimental	Analytical
10	0.927	0.891
20	1.853	1.782
30	2.780	2.673
40	3.707	3.564
50	4.710	4.455

Table 3: Cc Beams' Stress Values

Load (KN)	Maximum Stress (mm)
10	77.93
20	55.86
30	233.78
40	311.71
50	389.64

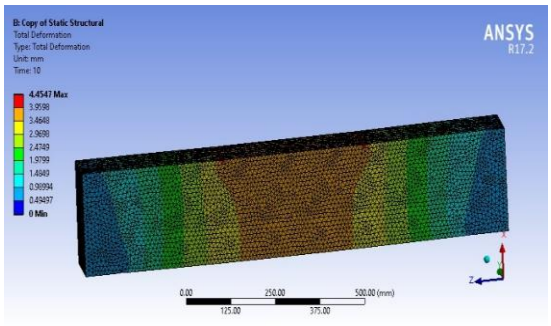

Fig. 4 (a): Conventional concrete beam deformation at 50 kN

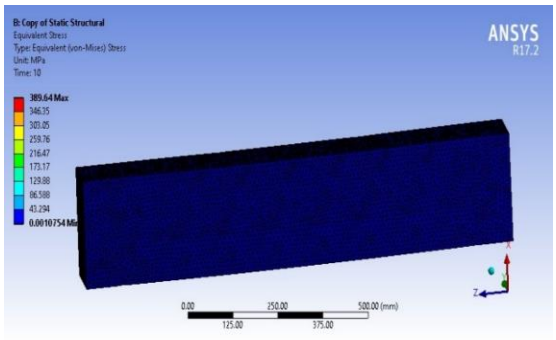

Fig. 4 (b): Conventional concrete beam stress of 50 kN

Tables 4 and 5 display the 10E (10% EPS) mix concrete beam's maximum deflection and stress values. The beam model's deformation and stress behavior at 50kN are shown in Figure 5(a&b). The experimental deflection value of 10E mix is 6.1%, 6.2%, 5%, 6.8% & 4% higher than the analytical value at 10, 20, 30, 40 & 50 kN load respectively. The stress value increased from 76.34mm at 10kN to 381.69mm at 50kN.

Table 4: 10e Mix Concrete Beams' Load-Deflection Values

Load (KN)	Max. deflection (mm)	
	Experimental	Analytical
10	0.912	0.859
20	1.826	1.719
30	2.712	2.579
40	3.675	3.438
50	4.469	4.297

Table 5: The 10e Mix Concrete Beams' Stress Values

Load (KN)	Maximum Stress (mm)
10	76.34
20	152.68
30	229.01
40	305.35
50	381.69

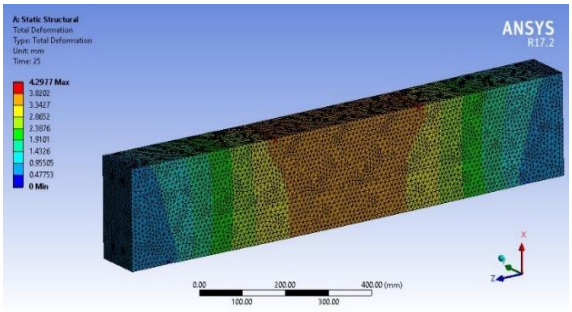

Fig. 5 (a). Deformation of a concrete beam with a 10E mix at 50 kN

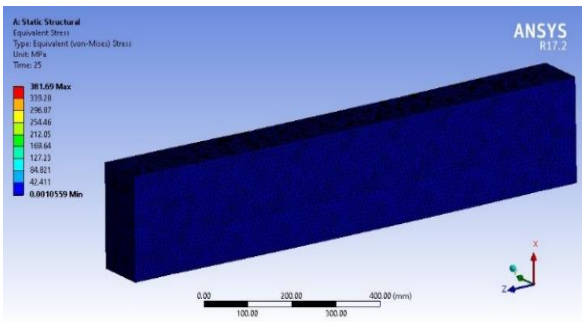

Fig. 5 (b). Stress of 10E mix concrete beam at 50 kN

The highest stress and deflection values for the 2M10E (2% MMT & 10% EPS) mix concrete beam are presented in Tables 6 and 7. The beam model's deformation and stress behaviour at 50kN are shown in figure 6 (a&b). A minor variation between the experimental and analytical values may be seen in table 6. The experimental and analytical values varied by 0.06 mm at 10 kN, 0.081 mm at 20 kN, 0.09 mm at 30 kN, 0.142 mm at 40 kN, and 0.349 mm at 50 kN. The stress value is also increased from 70.78mm to 353.94 mm.

Table 6: 2m10e-Mix Concrete Beams' Load-Deflection Values

Load (KN)	Max. deflection (mm)	
	Experimental	Analytical
10	0.815	0.755
20	1.592	1.511
30	2.357	2.266
40	3.163	3.021
50	4.125	3.776

TABLE 7: The 2M10E Mix Concrete Beams' Stress Values

Load (KN)	Maximum Stress (mm)
10	70.78
20	141.58
30	212.36
40	283.15
50	353.94

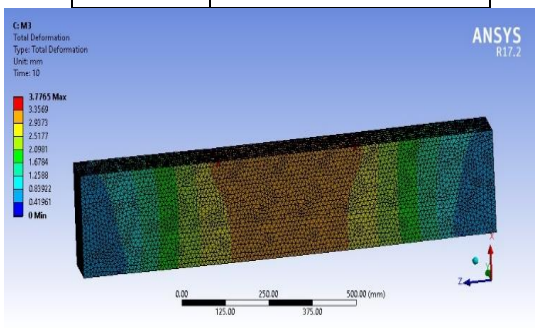

Fig. 6 (a). Concrete beam with 2M10E mix deformation at 50 kN

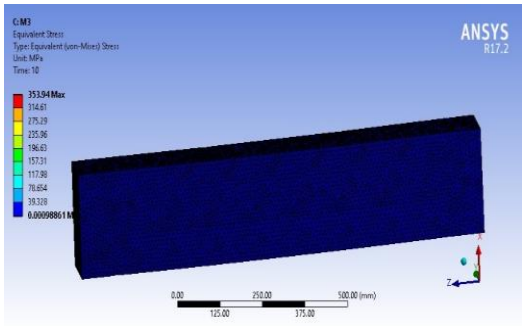

Fig. 6 (b). Stress of 2M10E mix concrete beam at 50 kN

Tables 8 and 9 show the stress value and maximum deflection value for the 4M10E (4% MMT & 10% EPS) mix concrete beam. Figure 7 (a&b) illustrates the deformation and stress behaviour of the beam model at 50kN. Compare to all other mixes 4M10E mix shows minimum deflection value and minimum stress value in both experimental and analytical. The ratio of experimental to analytical in 4M10E mix beams is 1.04:0.96 at 10kN, 1.08:0.92 at 20kN, 1.06:0.94 at 30kN, 1.09:0.92 at 40kN, and 1.07:0.93 at 50kN.

Table 8: 4m10e Mix Concrete Beams' Load-Deflection Values

Load (KN)	Max. deflection (mm)	
	Experimental	Analytical
10	0.702	0.675
20	1.465	1.351
30	2.148	2.027
40	2.951	2.703
50	3.623	3.378

TABLE 9: THE 4M10E MIX CONCRETE BEAMS' STRESS VALUES

Load (KN)	Maximum Stress (mm)
10	66.23
20	132.46
30	198.7
40	264.93
50	331.16

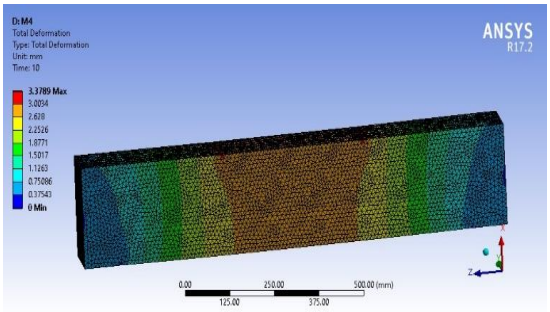

Fig. 7 (a). Deformation of concrete beam made of 4M10E mix at 50 kN

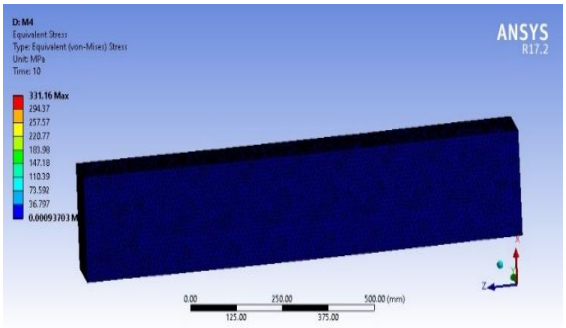

Fig. 7 (b). Stress of 4M10E mix concrete beam at 50 kN

According to the ANSYS beam model study, the mixes of CC, 10E, 2M10E, and 4M10E exhibited deflections of 4.455mm, 4.297mm, 3.776mm, and 3.378mm and stress of 389.64mm, 381.69mm, 353.94mm, and 331.16mm, respectively, for ultimate loads of 10 kN, 20 kN, 30 kN, 40 kN, and 50 kN. When EPS and MMT are added to concrete beams, the deflection and stress rate are decreased compared to standard concrete beams.

B. Load vs Deflection graph of beams

This section compares the findings from the experimental and analytical research of beams.

Based on analytical and experimental data, a load vs. deflection graph for the beams was created and presented in Figs. 8 through 11.

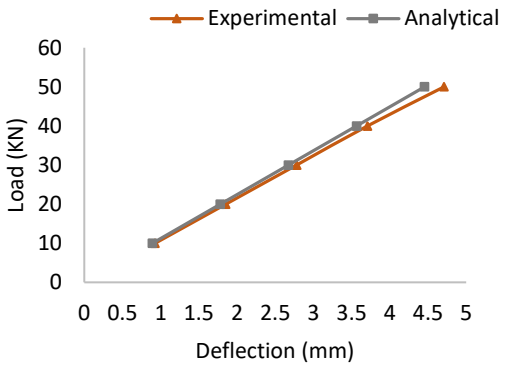

Fig. 8. Load vs Deflection graph of Control Beam

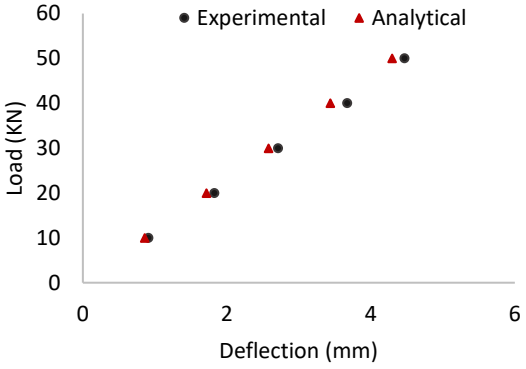

Fig. 9. Load vs Deflection graph of 10E mix composite Beam

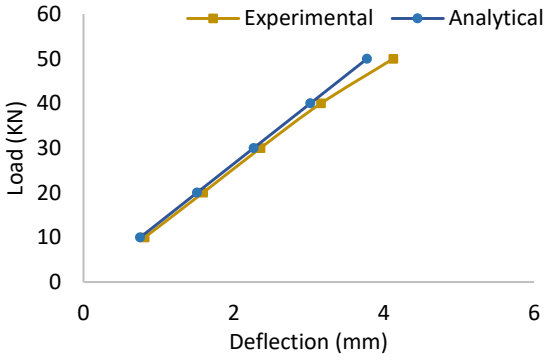

Fig. 10. Load vs Deflection graph of 2M10E mix composite Beam

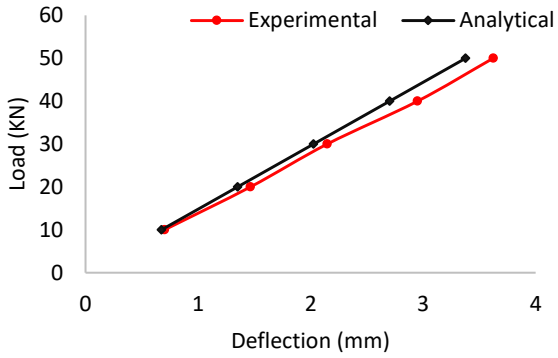

Fig. 11. Load vs Deflection graph of 4M10E mix composite Beam

Compared to the beam that has been empirically studied, the finite element model is stiffer due to the bond behaviour and composite action between different material components. Nonetheless, the composite action and binding behaviour between the two materials are thought to be imperfect since there is a possibility of slippage between the concrete and steel in an experimental beam. The application of stress and the development of fractures can potentially affect the bonding between concrete and steel material. However, the examined mid-span deflection values of LWC mixes were more in line with the findings from the analytical results because to the enhanced bonding capacity and interlocking of binder matrices with aggregate and steel reinforcement in beam specimens.

During the specimen analysis using ANSYS, fracture patterns and the most affected region were evaluated in order to assess the flexural failure of the RLWC beams. The most affected area (the orange area in Figures 5 to 7) was clearly visible between two-point loads, according to the examination of RLWC beam models. It is clear from doing flexural analysis on each beam model that the bigger fractures mostly occurred between the affected region (i.e., between two-point stresses). However, the flexural study of RLWC beams clearly demonstrated that the replacement of EPS as coarse aggregate and MMT as cement minimized the formation of cracks and their widths.

5. Conclusion

The ANSYS program was utilized to conduct a numerical analysis of the nonlinear behavior of

lightweight reinforced steel fiber beams under flexure. The outcomes are contrasted with those from the experiment. The load bearing capacity and load deflection characteristics of the analytical result were found to be lower than those of the experimental result. The results thus demonstrate that the mid-span deflection values of the LWC mixtures under investigation were more consistent with the conclusions of the ANSYS-based analytical beam models. Consequently, it can be said that there is an acceptable level of uniformity between the study's conclusions and the finite element analysis's findings.

REFERENCE

[1] A. Dd Figueiredo, M.R. Ceccato, "Workability analysis of steel fiber reinforced concrete using slump and Ve-Be test", Mater. Res. vol. 18, pp. 1284–1290, 2015.

[2] F.G. Cunha, Z. Sampaio, A. Martinelli, "Fiber-reinforced lightweight concrete formulated using multiple residues", Constr. Build. Mater. vol. 308, 125035, 2021.

[3] L. Huang, J. Xie, L. Li, B. Xu, P. Huang, Z. Lu, "Compressive behaviour and modelling of CFRP-confined ultra-high-performance concrete under cyclic loads", Constr. Build. Mater. vol. 310, 124949, 2021.

[4] M. Hassanpour, P. Shafigh, H.B. Mahmud, "Lightweight aggregate concrete fiber reinforcement–a review", Constr. Build. Mater., vol. 37, pp. 452–461, 2012.

[5] B. Zhang, et al., L. Li, "Effects of fibres on ultra-lightweight high strength concrete: dynamic behaviour and microstructures", Cem. Concr. Compos. Vol. 128, 104417, 2022.

[6] Abdeliazim Mustafa Mohamed, Bassam A. Tayeh, Yazan I. Abu Aisheh, Musab Nimir Ali Salih, "Exploring the performance of steel fiber reinforced lightweight concrete: A case study review", Case Studies in Construction Materials, Volume 18, ISSN 2214-5095, 2023.

[7] Md. Imran Kabir, C.K. Lee, Y.X. Zhang," Numerical and analytical investigations of flexural behaviours of ECC–LWC encased steel beams", Engineering Structures, Volume 239, ISSN 0141-0296, 2021.

[8] B.A. Solahuddin, "Strengthening of reinforced concrete with steel fibre: a review", Mater. Sci. Forum, pp. 81–86, 2022.

[9] B.A. Solahuddin, F.M. Yahaya, "A state-of-the-art review on experimental investigation and finite element analysis on structural behaviour of fibre reinforced polymer reinforced concrete beams", Heliyon, vol. 9 (3), e14225, 2023.

[10] Y. Zhu, Y. Zhang, H.H. Hussein, G. Chen, "Flexural strengthening of reinforced concrete beams or slabs using ultra-high-performance concrete (UHPC): A state-of-the-art review", Eng. Struct., vol. 205, 110035, 2020.

[11] T.M. Khaleel, M.H. Al-Sherrawi, "Shear strength of steel fibre RC beams under repeated loads", Mater. Today.: Proc., vol. 60, pp. 1808–1813, 2022.

[12] J. Li, J. Chen, C. Wan, J. Niu, "Flexural toughness and evaluation method of steel fiber reinforced self-compacting lightweight aggregate concrete", Constr. Build. Mater. Vol. 277, 122297, 2021.

[13] Gou H, Zh u H, Zhou H, Yang Z. "Reinforcement mechanism of orientally distributed steel fibers on ultra -high -performance concrete". Constr Buil d Mater., vol. 28 (1), 122646, 2021.

[14] Mohamed S. Manharawy, Ahmed A. Mahmoud, Osama O. El-Mahdy, Mosaad H. El-Diasity, "Experimental and numerical investigation of lightweight foamed reinforced concrete deep beams with steel fibers", Engineering Structures, Volume 260, ISSN 0141-0296, 2022.

[15] M. Alshannag, A. Charif, A. Alqarni, S. Nasser, "Flexural performance and ductility of RC beams made using natural LWA", Case Stud. Constr. Mater., vol. 16, e00942, 2022.

[16] S. A. Mohammed and A. I. Said, "Analysis of concrete beams reinforced by GFRP bars with varying parameters" Journal of the Mechanical Behavior of Materials, vol. 31, no. 1, pp. 767–774, 2022

[17] S. Mehany, H. M. Mohamed, and B. Benmokrane, "Flexural Strength and Serviceability of GFRP-Reinforced Lightweight Self-Consolidating Concrete Beams" Journal of Composites for Construction, vol. 26, no. 3, 2022.

[18] Touhami Tahenni, Farid Bouziadi, Bensaid Boulekbache, Sofiane Amziane, "Experimental and numerical investigation of the effect of steel fibres on the deflection behaviour of reinforced concrete beams without stirrups", Structures, Volume 33, Pages 1603-1619, 2021.

[19] Mohammad Alshannag, Mansur Alshmalani, Abdulaziz Alsaif, Mahmoud Higazey, "Flexural

performance of high-strength lightweight concrete beams made with hybrid fibers", Case Studies in Construction Materials, Volume 18, ISSN 2214-5095, 2023.

[20] Al-Naimi, H.K., Abbas, A.A. "Structural Behaviour of Steel-Fibre-Reinforced Lightweight Concrete. Improvements and Innovations" BEFIB 2020. RILEM Bookseries, vol 30. Springer, 2021.

[21] Mohamed A. El Zareef "An Experimental and Numerical Analysis of the Flexural Performance of Lightweight Concrete Beams reinforced with GFRP Bars", Engineering, Technology & Applied Science Research Vol. 13, No. 3, pp 10776-10780, 2023.

[22] Ghannoum M, Abdelkhalek L, Assaad JJ. "Application of Stochastic Finite Element Modeling to Reinforced Lightweight Concrete Beams Containing Expanded Polystyrene Beads", Buildings, vo. 13(9), 2294, 2023.

[23] Alzara, Majed, Riad, Magdy, AbdelMongy, Mohamed, Farouk, Mohamed A., Yosri, Ahmed M., Moubarak, Ahmed M., Ehab, Ahmed, "Analysis of Lightweight Polystyrene Foam Concrete Flat Slabs under Fire Condition", Advances in Civil Engineering, 1964903, 2022.

[24] Ibrahim G. Shaaban, Amr H. Zaher, Mohamed Said, Wael Montaser, Mohamed Ramadan, Ghada N. Abd Elhameed, "Effect of partial replacement of coarse aggregate by polystyrene balls on the shear behaviour of deep beams with web openings", Case Studies in Construction Materials, Volume 12, ISSN 2214-5095, 2020.

[25] Xi Liu, Yijia Sun, Tao Wu, Yang Liu, "Flexural cracks in steel fiber-reinforced lightweight aggregate concrete beams reinforced with FRP bars", Composite Structures, Volume 253, ISSN 0263-8223, 2020.

[26] Chandramouli P, Muthukrishnan D, Sridhar V, Sathish Kumar V, Murali G, Vatin NI. "Flexural Behaviour of Lightweight Reinforced Concrete Beams Internally Reinforced with Welded Wire Mesh", Buildings, vol. 12(9), 1374, 2022.

[27] Al Zand, A.W.; Alghaaeb, M.F.; Liejy, M.C.; Mutalib, A.A.; Al-Ameri, R. "Stiffening Performance of Cold-Formed C-Section Beam Filled with Lightweight-Recycled Concrete Mixture", Materials, vol. 15, 2982, 2022.